Targeting Positive Cofactor 4 induces autophagic cell death in MYC-expressing diffuse large B cell lymphoma

Le Ma
Third Military Medical University: Army Medical University https://orcid.org/0000-0002-1811-2639
Qiang Gong
Third Military Medical University: Army Medical University
Zelin Chen
Third Military Medical University: Army Medical University
Yu Wang
Third Military Medical University: Army Medical University
Xu Tan
Third Military Medical University: Army Medical University
Yunsheng Liu
Third Military Medical University: Army Medical University
Yawei Wang
Third Military Medical University: Army Medical University
Gaoyu Liu
Third Military Medical University: Army Medical University
Jianlin Fu
Third Military Medical University: Army Medical University
Mingling Xie
Third Military Medical University: Army Medical University
Peng Luo
Third Military Medical University: Army Medical University
Jieping Chen
Third Military Medical University: Army Medical University
Chunmeng Shi (shicm@tmmu.edu.cn)
Third Military Medical University: Army Medical University https://orcid.org/0000-0002-8264-738X

Research

Keywords: Positive Co-factor 4, Diffuse large B-cell lymphoma, Autophagic cell death, c-Myc, Aerobic glycolysis

Posted Date: April 21st, 2021

DOI: https://doi.org/10.21203/rs.3.rs-421070/v1

Abstract

Background: The MYC-expressing diffuse large B-cell lymphoma (DLBCL) is one of the refractory lymphomas. The pathogenesis of MYC-expressing DLBCL is still unclear, and there is a lack of effective therapy. In this study, we have explored the clinical significance and the molecular mechanisms of transcription co-activator 4 (PC4) in MYC-expressing DLBCL.

Methods: We investigated PC4 expression in 54 cases of DLBCL patients' tissues and matched normal specimens, and studied the molecular mechanisms of PC4 in MYC-expressing DLBCL both in vitro and in vivo.

Results: We reported for the first time that targeting c-Myc could induce autophagic cell death in MYC-expressing DLBCL cell lines. We next characterized that PC4 was an upstream regulator of c-Myc, and PC4 was overexpressed in DLBCL and was closely related to clinical staging, prognosis and c-Myc expression. Further, our in vivo and in vitro studies revealed that PC4 knockdown could induce autophagic cell death of MYC-expressing DLBCL. And inhibition of c-Myc mediated aerobic glycolysis and activation of AMPK / mTOR signaling pathway were responsible for the autophagic cell death induced by PC4 knockdown in MYC-expressing DLBCL. Through the CHIP, DLRTM and EMSA assay, we also found that PC4 exerted its oncogenic functions by directly binding to c-Myc promoters.

Conclusions: PC4 exerts its oncogenic functions by directly binding to c-Myc promoters. Inhibition of PC4 can induce autophagic cell death of MYC-expressing DLBCL. Our study provides novel insights into the functions and mechanisms of PC4 in MYC-expressing DLBCL, and suggests that PC4 might be a promising therapeutic target for MYC-expressing DLBCL.

Background

Diffuse large B-cell lymphoma (DLBCL) is the most common subtype of adult non-Hodgkin lymphoma with tremendous heterogeneity in terms of clinical manifestations, histological morphology and prognosis[1,2]. Rituximab in the combination with CHOP chemotherapy (R-CHOP) is the standard therapeutic regimen for DLBCL, but nearly 40% of patients have a poor prognosis due to recurrence and drug resistance, while only 10% of patients can be completely cured[2]. According to previous studies, most patients show chromosomal abnormalities, including the translocation and amplification of c-Myc, Bcl-2 and Bcl-6 genes[3-5]. Among them, MYC-expressing DLBCL is one of the refractory lymphoma with unclear pathogenesis, rapid progression, chemo-resistance and low cure rate, which is an urgent problem to be solved[6-7]. However, c-Myc is a natural disordered protein and lacks drug recognition sites, presenting a significant challenge for drugs targeting c-Myc and thus showed side effects. Therefore, the development of anti-tumor drugs targeting c-Myc is challenging and exhibits various hurdles[8].

The c-Myc is an oncogene, which not only regulates tumor growth and differentiation, but also is a key regulator in energy metabolism, indicating a crucial therapeutic target for DLBCL[9]. In recent years, a

promising phenomenon has been found in the study of tumor energy metabolism, the rapid reduction of the energy charge below a critical limit can trigger autophagy cell death rather than an adaptive autophagic response[10]. Different from apoptosis (Type I programmed cell death), autophagic cell death (Type II programmed cell death) occurs in various types of cancer[11]. In previous studies, inhibition of MYC could induce autophagic cell death in Burkitt lymphoma cell lines[12], but the specific mechanism was unclear. The combination of the antidepressants maputiline and fluoxetine induce autophagic cell death in drug-resistant Burkitt's lymphoma[13]. In multiple myeloma, metformin can induce autophagic cell death through the AMPK/mTOR pathway[14-15]. This type of cell death can have a contribution to anticancer efficacy or drug resistance, respectively[16,17]. Therefore, targeting autophagy may provide a new potential therapeutic strategy to overcome drug resistance[18].

In this study, we firstly revealed that targeting c-Myc would induce autophagic cell death in MYC-expressing DLBCL cell lines. Through bioinformatics analysis, we found that PC4 was abnormally high expressed in DLBCL and was positively correlated with MYC expression. Considering the key role of c-Myc in DLBCL, it is crucial to elucidate the potential role and underlying molecular mechanisms of PC4 in DLBCL. Then, we first reported that PC4 was highly expressed in DLBCL, and positively correlated with c-Myc expression and poor prognosis of patients. Next, our findings revealed that PC4 knockdown induced autophagic cell death in MYC-expressing DLBCL, which is a new type of cell death. Surprisingly, knockdown of PC4 had no significant influence on the c-Myc low expression cell lines and non-cancerous lymphocytic cell lines. We also found that inhibition of c-Myc mediated aerobic glycolysis and excessive activation of the AMPK / mTOR signaling pathway were responsible for the autophagic cell death induced by PC4 knockdown in MYC-expressing DLBCL. Furthermore, PC4 exerted its oncogenic functions by directly binding to c-Myc promoters. Our study provides novel insights into the functions and mechanisms of PC4 in MYC-expressing DLBCL, and suggested that PC4 might be a promising therapeutic target for MYC-expressing DLBCL.

Methods

Cell lines and clinical samples

The human lymphocytic cell lines (CCRF-SD) and diffuse large B-cell lymphoma cell lines (DOHH2, OCL-LY10, HBL-1 and TMD8) were purchased from the Cell Bank of the Chinese (Shanghai, China). All cells were cultured in the RPMI-1640 medium (Hyclone, USA), supplemented with 1% streptomycin/penicillin (Beyotime, Shanghai, China) and 10% FBS (Gibco, USA), and incubated at 37°C with 5% CO_2. A number of 24 DLBCL patients' RNA samples and 24 normal lymph gland RNA samples and a total of 30 paraffin-embedded DLBCL patients' tissues with paired adjacent tissues were obtained at Department of Hematology of Southwest Hospital of Third Military Medical University. All DLBCL patients were diagnosed by Lymph node biopsy and confirmed diagnosis by at least two experienced pathologists. The study was approved by the Ethics Committee of Third Military Medical University.

Animals

4-5 weeks old male athymic nude mice were obtained from the Center and followed the care and use of Guidelines from Laboratory Animals of the TMMU. Nude mice were kept in a specific pathogen-free condition and all experimental procedures were approved by the TMMU Animal Care and Use Committee.

Immunohistochemical Staining

The paraffin-embedded patients' tissues were dewaxed and rehydrated and incubated with human PC4 antibody (1: 200; Sigma, St. Louis, Missouri, USA) at 4°C overnight. Then, the slides were sequentially incubated with secondary antibody at 37°C for 1hour, and used DAB to visualize positive staining. PC4 expression in DLBCL patients' tissues was evaluated by percentage of positive-staining cells. Intensity was graded as follows: 0, no signal; 1, weak (light yellow); 2, moderate (brown); and 3, strong staining. The percentage of positive cells was evaluated quantitatively and scored as: 0 (< 5% positive tumor cells), 1 (5–25% positive tumor cells), 2 (26–50% positive tumor cells), 3(51–75% positive tumor cells) and 4 (> 75% positive tumor cells). The final quantification of each staining was obtained by multiplying these 2 scores. A total staining score of 0–12 was calculated and graded as negative (–, score 0–1), weak (+, score 2–4), moderate (++, score 5–8), or strong (+++, score 9–12).

Quantitative RT-PCR

Total RNA was collected from DLBCL cells using Trizol (Cwbiotech, China). 1μg RNA was reverse transcribed into cDNA according to the recommended protocol by the RevertAid First Strand cDNA Synthesis kit. (#K1622, Thermo Fisher Scientific, Inc.) Quantitative RT-PCR was performed according to the recommended protocol by SYBR Green qPCR master mix (Takara). When the reactions were completed, the relative gene expression was calculated by the comparative threshold cycle (Ct) method. GAPDH expression was used as control. Human-specific primers sequences are shown in Additional file 1: Table S1.

RNA interference

The shRNA lentivirus vector targeting human PC4(shPC4#1:5'-GACAGGUGAGACUUCGAGATT -3'; 5'-UCUCGAAGUCUCACCUGUCTT -3'.shPC4#2:5'-ACAGAGCAGCAGCAGCAGATT-3';5'-UCUGCUGCUGCUGCUCUGUTT-3') ; and c-Myc(sh-c-Myc#1:5'-ATGTCAAGAGGCGAACACA-3';5'-TGTGTTCGCCTCTTGACAT-3'.sh-c-Myc#2:5'-ACGATTCCTTCTAACAGAAAT-3';5'-ATTTCTGTTAGAAGGAATCGT-3'.) negative control shRNA(5'-UUCUCCGAACGUGUCACGUTT-3';5'-ACGUGACACGUUCGGAGAATT-3') were purchased and constructed by GenePharma (Shanghai, China). The human PC4 plasmid and control were purchased and constructed from GeneChem (Shanghai, China). The human GLUT1 plasmid were purchased and constructed from GenePharma (Shanghai, China). GFP-LC3 plasmid was purchased and constructed from Addgene and siRNA targeted to Atg7 was purchased and constructed by GeneChem (Shanghai, China). TMD8 and HBL-1 cells were transfected with shRNA or plasmid according to the recommended instructions. PC4 and c-Myc binding site mutation was conducted by Cas9-sgRNA co-expressed plasmids according to the instruction. Binding site wild type sequence: CCAACAAATGCAATGGGAGT.Binding site mutation sequence: TTGGTGGGCATGGCAAAGAC.

Cell proliferation assay

Cells were cultured in 96-well plates with a density of 3000 cells each well and 100 ul RPMI-1640 medium. Cellular proliferation was measured with the Cell Counting Kit-8 (Dojindo, Japan) at the wavelength of 450 nm. Data were read by a microplate reader (Multiskan Go Multimode Reader; Thermo Scientific).

Cell apoptosis analysis by flow cytometry

Cells were treated with AnnexinV- 7-AAD (BD Biosciences) for 30 min at 37°C in the dark for apoptosis analysis, then analyzed by flow cytometry.

Western blotting analysis

The cell lines were harvested, washed, and lysed with RIPA buffer (Beyotime, China) which contain protease inhibitor cocktail (Roche) for 30min on ice. Total protein was collected and quantitated by a BCA kit (Beyotime, China) according to the recommended instruction. The protein samples were separated by electrophoresis in gel, and then transferred onto PVDF membranes (Millipore). Blotted membranes were incubated with primary antibodies overnight at 4°C. The membranes were washed 5min for 3 times with TBST, and then incubated with HRP-linked secondary antibody (Cell Signaling Technology, USA) 1h at room temperature. The band intensities were detected and visualized by an enhanced chemiluminescence detection system (Bio-Rad Laboratories). Primary antibodies against c-Myc, LC3, SQSTM1,ATG7,PARP,CASPASE3,Bcl-2,BAX,PI3K,S6K1,AKT,mTOR,4EBP1,AMPK,P38,P53,HIF-1α,GLUT1,PKM2,HK2,LDHA and β-actin were obtained from Cell Signaling Technology. Primary antibodies against PC4 were obtained from Sigma.

Immunofluorescence staining

Cells were fixed in 4.0% formaldehyde for 10 min and permeabilized with ice-cold methanol or 0.5% Triton X-100 for 5 min. The following primary antibodies were used, and subsequently using secondary antibodies to detect Primary antibodies. Conjugating to AlexaFluor 488 or 555(Invitrogen). Cells were counterstained with DAPI and mounted in Vectashield (Vector Laboratories).

In vivo tumor growth model

For in vivo tumor growth model, 100 ul PBS containing $1x10^7$ PC4 stable knockdown TMD8 cells or negative control cells or controls were injected subcutaneously at one dorsal site of athymic male nude mice. Tumor growth was measured every 2 days, which was calculated by the following formula: volume (mm^3) = ($width^2$ * length)/2. At the endpoint, the mice were sacrificed, and then xenografts were dissected, weighed and fixed in 4% paraformaldehyde.

ECAR, glucose uptake, lactate and ATP assays

Extracellular acidification rate (ECAR) was measured using extracellular flux analyzer (XFp) analyzer (Seahorse Bioscience) according to the recommended instructions. Lactate production (Lactate Assay Kit) was measured according to the manufacturer (BioVision). For glucose uptake analyse, cells were cultured with a fluorescent D-glucose derivative, 2-[N-(7-nitrobenz-2-oxa-1, 3-diazo-l-4-yl)amino] -2-deoxy-D-glucose (2-NBDG; APExBIO) for 30min at 37 °C. The fluorescence intensity of 2-NBDG was measured through flow cytometry (BD FACSCanto II™). ATP production (Enhanced ATP Assay Kit) was measured according to the recommended manufacturer's protocol (Beyotime).

Transmission electron microscopy

Cells were harvested and immediately fixed in 3% glutaraldehyde overnight at 4°C and postfixed with 2% osmium tetroxide for 1 hour at 37°C. And then, cells were embedded and stained using uranylacetate/lead citrate. The samples were imaged using a TEM (JEM-1400PLUS, Japan).

Colony formation assay

For colony formation assay, Firstly, we used 0.5%gelatin soaked plates for 20minutes, then sucked the gelatin, adding lymphoma cells cultured for 6-8hours to adherence to the plates. TMD8 and HBL-1 cells were collected and seeded in 6-well plates. Cells were cultured up to 14 days until colonies were clearly visible, the medium was changed every two days. At the endpoint, cells were washed twice with PBS, and then fixed with 4% paraformaldehyde, stained with crystal violet (Beyotime, China) for 30 min, and colonies were counted (more than 50 cells).

RNA-seq assay

Total RNA was extracted using Trizol reagent (Invitrogen, CA, USA) following the manufacturer's procedure. The total RNA quantity and purity were analysis of Bioanalyzer 2100 and RNA 6000 Nano LabChip Kit (Agilent, CA, USA) with RIN number >7.0.Approximately 10 ug of total RNArepresenting a specific adipose type was subjected to isolate Poly (A) mRNA with poly-T oligoattached magnetic beads (Invitrogen). Following purification, the mRNA is fragmented into smallpieces using divalent cations under elevated temperature. Then the cleaved RNA fragments werereverse-transcribed to create the final cDNA library in accordance with the protocol for the mRNASeqsample preparation kit (Illumina, San Diego, USA), the average insert size for the paired-endlibraries was 300 bp (±50 bp). And then we performed the paired-end sequencing on an Illumina sequence platform.

Luciferase reporter assay

TMD8 cells were cultured at a density of 5×10^4 cells/well in 96-well culture plates and transfected with 0.2 μg of dual-luciferase reporter construct SUB1, or co-transfected with 0.2 μg of the luciferase reporter construct c-Myc and the internal control vector pRL-TK, pRL-SV40, or pRL-CMV (Promega, Madison, WI) at a ratio of 20:1 (reporter construct: control vector) using LipofectamineTM 2000 (Invitrogen, Carlsbad, CA) according to instruction of the recommended manufacturer.

Chromatin immunoprecipitation (ChIP-PCR)

TMD8 cells were conducted ChIP assay with the SimpleChIP Enzymatic Chromatin IP Kit (Magnetic Beads) (#9003; Cell Signaling Technology) according to the recommend manufacturer's instructions. Chromatin fragments were immunoprecipitated with anti-PC4 (NB10059774; Novus Biologicals), or rabbit IgG (#2729; Cell Signaling Technology) coupled with ChIP Grade Protein G Magnetic Beads (#9006; Cell Signaling Technology).

EMSA (electrophoretic mobility shift assay)

The DNA binding assays were performed using purified GST-PC4 protein and biotin-labelled fragments of the promoters containing the W-boxes, using GST protein as a negative control, and non-labeled fragments were used as competitors. The bands at the upper and lower part of membranes indicate shift (protein-probe complex) and unbound free probes, respectively.

Statistical analysis

Statistical analysis was carried out using SPSS 22.0 software (SPSS Inc., Chicago, USA), and all data were presented as means ± SD. Comparisons between two groups were performed using the Student's t-test. Comparisons among three or more groups were performed using a one-way analysis of variance (ANOVA). The survival data was carried out using the Kaplan-Meier method. Correlation between PC4 expression and clinical parameters was determined using the Pearson's χ^2 method. $P < 0.05$ indicated a statistically significant difference.

Results

PC4 is highly expressed in DLBCL and positively correlated with c-Myc expression and poor prognosis of patients.

We began our studies by exploring the potential clinical significance of PC4, we firstly analyzed PC4 expression level in DLBCL specimens compared with their adjacent normal tissues. As shown in Figure 1A, high levels of PC4 were detected in tumor tissues, while the adjacent normal tissues had a low level of PC4. The average staining score of PC4 expression confirmed the above results. We also analyzed GEPIA database and revealed that PC4 was positively correlated with MYC expression ($P<0.001, R=0.46$) in human whole blood (Supplemental Figure 1A). Moreover, GEPIA database showed that PC4 mRNA expression level was significantly higher in DLBCL patients tissues (n=47) than in normal tissues (n=337) (Supplemental Figure 1B). Then, we analyzed PC4 expression in DLBCL specimens with or without positive expression of c-Myc protein, and found that average staining score of PC4 in c-Myc(+) tissues were significantly increased compared to c-Myc(-) tissues (Figure 1B). In addition, we evaluated PC4 mRNA expression level in tumor tissues compared with normal tissues (Figure 1C), the mRNA expression of PC4 in tumor was apparently higher than that in normal tissues. Moreover, We analyzed PC4 mRNA expression level and found that c-Myc(+) tissues had higher PC4 mRNA expression compared to c-Myc(-)

tissues (Figure 1D). The data above suggested a possible positive correlation between PC4 expression levels and c-Myc expression level in DLBCL. Meanwhile, through analyzing 159 and 414 cases of DLBCL from public cancer databases (GSE4475 and GSE10846, respectively) we found that the higher PC4 expression group had poorer overall survival compared with lower PC4 expression group (Figure 1E and 1F). Although c-Myc expression demonstrated no significant change on the basis of gender, age, subtype, Ki-67 expression, it had poorly differentiated in DLBCL with a higher Ann Arbor stage and poorly event-free survival (Table1). Finally, we detected the protein level of PC4 and c-Myc in non-cancerous lymphocytic cell lines (CCRF-SD) and DLBCL cell Lines (DOHH2, OCL-LY10, HBL-1 and TMD8), our result showed that PC4 and c-Myc expression were much higher in TMD8 and HBL-1 cells compared to other cell lines (Figure 1G). The qPCR (Figure 1H) and Immunofluorescent staining (Supplemental Figure 2A) assays confirmed that the mRNA and protein level of PC4 was up-regulated in DLBCL cell lines (DOHH2, OCL-LY10, TMD8 and HBL-1 cells) compared with non-cancerous lymphocytic cell lines (CCRF-SD cells). Collectively, these results suggest that PC4 is a potential oncogene and positively correlated with c-Myc in DLBCL.

Knockdown of PC4 induces cell apoptosis in MYC-expressing DLBCL in vitro and in vivo.

To investigate the functional significance of increased PC4 expression in DLBCL, TMD8 and HBL-1 cells were used for the subsequent loss-of-function study. The stable cell lines with PC4 knockdown were established by specific shRNA (shPC4#1 and shPC4#2) (Figure 2A). The CCK-8 assays demonstrated that PC4 knockdown inhibited the proliferation (Figure 2B). Then, the expression of apoptosis protein markers, including poly ADP-ribose polymerase (PARP), cleaved caspase 3, B-cell lymphoma-2 (BCL-2) and B-cell lymphoma-2-Associated X (BAX) were detected by western blotting in the constructed cells (Figure 2C). As shown in Figure 2D, knockdown of PC4 increased apoptosis in stable PC4 Knockdown cell lines than controls, Gene Set Enrichment Analysis (GSEA) showed that the gene sets of apoptosis enrichment in PC4 low (shPC4) in TMD8 cell lines (Figure 2E), which means that PC4 silencing can induce cell apoptosis. Knockdown of PC4 also inhibited the colony formation capacity in TMD8 and HBL-1 cells (Figure 2F). We observe cell vacuoles and cell debris in the constructed cells through a microscope (Supplemental Figure 3A). Moreover, TEM images showed autophagic vacuole (AV) formation in the constructed cells (Figure 2G). These finding suggested that knockdown of PC4 was associated with autophagy. In addition, we established a subcutaneous xenograft model to study the biological function of PC4 in vivo. TMD8 cells with or without stable PC4-knockdown were inoculated into athymic male nude mice. During the in vivo experiments, xenograft growth in the sh-PC4#1 group was dramatically inhibited compared to the sh-NC group and control group (Figure 2I). The average tumor weight and tumors size at the experimental endpoint was reduced by PC4 knockdown (Figure 2H and 2J). Besides, knockdown of PC4 had no significant impact on mice body weight (Figure 2K). Furthermore, the down-regulation of PC4 induced the expression of c-PARP and the expression of the LC3II, which also decreased SQSTM1 (Figure 2L), indicating that knockdown of PC4 could induce apoptosis and autophagy in vivo. Taken together, the above data suggests that PC4 promotes DLBCL cell proliferation, and knockdown of PC4 can induce apoptosis and autophagy both in vitro and in vivo.

Knockdown of PC4 induces apoptosis in MYC-expressing DLBCL by inducing excessive autophagy.

Non-selective autophagy occurred due to lack of energy[11]. As envisioned, Silencing of PC4 could induce the expression of the LC3II and down-regulated the SQSTM1 protein in DLBCL cells (Figure 3A). We also detected the level of autophagy in all cell lines and found no significant differences between each other (Supplemental Figure 4A). The associated autophagy proteins (beclin1, ULK1, ATG7)also up-regulated after silencing of PC4 (Figure 3B). In addition, TEM images showed AV formation in PC4 knockdown cells, which could be reversed by 3-methyladenine (3MA; an autophagy inhibitor) (Figure 3C). Moreover, GFP-LC3 puncta were observed in the constructed cell lines and their presence was significantly inhibited by 3MA (Figure 3D). Above-mentioned data suggested that autophagy was induced by PC4-knockdown. PC4 knockdown significantly suppressed the proliferation of TMD8 and HBL-1 cells, which was partly reversed by 3MA (Figure 3E). Similarly, the cell apoptosis was also reversed by 3MA (Figure 3F). Moreover, the level of LC3II and cell apoptosis marker c-PARP partly reversed by 3MA (Figure 3G). We also used siRNA against ATG7 (Figure 3H). Intriguingly, the level of LC3II and c-PARP was significantly reversed by siATG7 (Figure 3I). The cell proliferation in the constructed cells were also reversed by siATG7 (Figure 3J). Therefore, our results confirmed that PC4 knockdown could induce autophagic cell death in TMD8 and HBL-1 cells. To assess the effect of knockdown of PC4 in c-Myc low expression cell lines (DOHH2 and OCL-LY10) and CCRF-SD were established with PC4 knockdown by specific shRNA (Supplemental Figure 4B). Interestingly, we found no effect on the level of LC3II and cleaved PARP and cell proliferation (Supplemental Figure 4C and 4D). Collectively, these results suggested that PC4 inhibition can induce autophagic cell death only in the c-Myc high expressing DLBCL cell lines. Galluzzi reported that a rapid reduction in energy charge below a critical limit is likely to trigger autophagic cell death[11]. This is well established that c-Myc is a key regulator in energy metabolism[9], suggesting that PC4 may directly regulate c-Myc or metabolism. This indicated that PC4 is a tumor-specific oncogene and may be a novel therapeutic target for MYC-expressing DLBCL.

Knockdown of PC4 induces excessive autophagy through AMPK/mTOR signaling pathway in MYC-expressing DLBCL.

We conducted Genome-wide analysis to compare the gene expression profiles in TMD8 with or without stable PC4-knockdown to explore the potential mechanism of PC4 on cell proliferation inhibition and apoptosis in DLBCL. The heat map showed that 4 genes, including c-Myc, reduced their expression, while the expression of 36 genes were increased after PC4 knockdown (Figure 4A). We identified 12669 potential PC4 target genes in TMD8 stable PC4 knockdown cells and 13,082 in control cells, with 12172 genes that overlap between TMD8 stable PC4 knockdown cells and control cells (Figure 4B). Then, we analyzed PC4 and c-Myc mRNA expression difference in stable PC4 knockdown TMD8 cells and controls cells (Figure 4C), our result showed that c-Myc significantly reduced after PC4 knockdown. In addition, We used KEGG enrichment analysis in TMD8 stable PC4 knockdown cells and controls (Figure 4D), which revealed that after PC4-knockdown AMPK signaling pathway was most increased and PI3K-Akt signaling pathway was most inhibited. Moreover, we established Gene ontology analysis to understand the PC4 full function, the results demonstrated that PC4 could positive regulate the metabolic process and cellular

process in DLBCL (Figure 4E). Therefore, PC4 promotes proliferation in DLBCL through regulating metabolism. According to the data from Genome-wide analysis, we established mTOR signaling pathway and downstream protein (4EBP1 and S6K1) by western blot, our result showed that the level of phosphorylation was decreased after PC4 knockdown (Figure 4F). Then we detected mTOR upstream signaling pathway including AMPK, P53, P38 and AKT, which revealed that the level of AMPK phosphorylation was comparatively more increased than the other proteins (Figure 4G). GSEA showed that the gene sets of mTORC1 were enriched in $PC4^{high}$ (Control) compared with $PC4^{low}$ (shPC4) in TMD8 cell lines (Figure 4L). For a deep insight into the role of PC4 in DLBCL, we next conducted related rescue experiment. The AMPK signaling pathway inhibitor Dorsomorphin (compound C) was used in the constructed cells (Figure 4H). Surprisingly, we found that the level of LC3II and c-PARP were partly reversed by Dorsomorphin in the constructed cells (Figure 4I and 4K). The cell proliferation was also partly reversed by Dorsomorphin (Figure 4J), indicating that the stress caused by PC4-knockdown negatively affect cell survival in DLBCL. A previous study showed that alteration of the above pathways was associated with energy metabolism declension[19]. Thus, we next conducted metabolism-related experiments.

Knockdown of PC4 induces excessive autophagy through inhibition of glycolysis metabolism in MYC-expressing DLBCL.

To further illustrate the underlying mechanisms of PC4 in DLBCL, we conducted metabolism-related experiments. We found that the 2-NBDG uptake and the production of Lactate and ATP were significantly inhibited after PC4-knockdown (Figure 5A, 5B and 5C). As expected, the extracellular acidification rate (ECAR), which reflected the overall glycolytic flux, also decreased in TMD8 stable PC4 Knockdown cell lines (Figure 5D). Furthermore, Silencing of PC4 inhibited the key enzymes of glycolysis including GLUT1, PKM2, HK2 and LDHA (Figure 5E). GSEA showed that the gene sets of glycolysis were enriched in $PC4^{high}$(Control) compared with $PC4^{low}$ (shPC4) in TMD8 cell lines (Figure 5K). To confirm the role of PC4 in glycolysis, we next over-expressed GLUT1 in stable PC4 Knockdown cell lines (Figure 5F). As expected, the cell viability (Figure 5H) and colony formation (Figure 5G) were partly reversed after over-expressed GLUT1. We found that the level of AMPK phosphorylation (Figure 5I) and the expression of c-PARP and LC3II (Figure 5J) were partly decreased by overexpression of GLUT1. These findings indicate that the stress caused by PC4-knockdown was associated with glycolysis metabolism.

PC4 directly regulates c-Myc transcription to perform it's oncogene function.

Previous studies showed that glycolysis metabolism was regulated by c-Myc[20] and HIF-1α[21]. Then we performed western blotting and q-PCR on c-Myc and HIF-1α and found that the protein and mRNA level of c-Myc was dramatically decreased in stable PC4 knockdown cell lines (Figure 6A and 6B). GSEA showed that the gene sets of MYC were enriched in $PC4^{high}$ (Control) compared with $PC4^{low}$ (shPC4) in TMD8 cell lines (Figure 6C). To further demonstrate the relationship between PC4 and c-Myc, we subsequently examined the relationship between PC4 and c-Myc. Schematic presentation of PC4 and c-Myc binding sites on the c-Myc locus are shown in Figure 7A,BS: binding site, BS1: CCAACAAATGCAATGGGAGT and

BS2: CAGGAGGGGCGGTATCTG. We conducted luciferase reporter assays, which revealed that PC4 regulated c-Myc transcription through two PC4 binding sites in c-Myc promoters (Figure 7B). However, EMSA and ChIP-PCR confirmed PC4 as a DNA binding protein, which is associated with the c-Myc binding sequence in BS1, not in BS2 (Figure 7C and 7D). To further verify the BS1 function, we conducted BS1 mutation in TMD8 and HBL-1 cell lines, BS mutation sequence: TTGGTGGGCATGGCAAAGAC. Our result confirmed that PC4 directly activate c-Myc transcription through BS1(Figure 7E, 7F and 7G). As expected, the protein and mRNA level of c-Myc both decreased in BS1 mutation cell lines (Figure 7F and 7G). In addition, the protein and mRNA level of PC4 has no significant influence after c-Myc stable knockdown (Supplemental Figure 5A and 5B). The results of the above experiments indicated that PC4 as the upstream gene of c-Myc, which directly regulated c-Myc transcription to perform its carcinogenic function.

Discussion

Owing to the increased recurrence and chemotherapy resistance, current strategies for the treatment of c-Myc (+) DLBCL are still facing with many difficulties and challenges[22]. And c-Myc is a natural disordered protein and lacks drug recognition sites that can be utilized[8]. Therefore, it is critical to identify the c-Myc related targets for precise individualized therapy and better prognosis. Here, we find a novel oncogene, PC4, which is overexpressed in DLBCL and positively correlated with c-Myc expression. Moreover, targeting PC4 can induce therapeutic autophagy by inhibiting c-Myc mediated aerobic glycolysis and activating AMPK / mTOR pathway in c-Myc (+) DLBCL. Interestingly, there is no significant effects on the c-Myc low expressing cells and non-cancerous lymphocytic cells after PC4 stable knockdown. These findings indicate that PC4 is a tumor-specific oncogene in c-Myc (+) DLBCL.

PC4 is a nuclear protein which also known as SUB1. As a multifunctional nuclear protein, PC4 is initially isolated, purified and identified from the upstream stimulatory activity (USA) in mammalian cell nuclear extracts[23-25]. Apart from its transcriptional co-activation function that facilitates RNA polymerase II-driven gene transcription[26-32], PC4 also plays an important role in various cellular process including DNA replication, DNA repair and chromatin organization[33-42]. PC4 also participated in the regulation of autophagy[43-45]. During the malignant transformation of normal dermal multipotent fibroblasts, we reported that PC4 is up-regulated and positively correlated with K-Ras and MAPK pathway, implying the potential role of PC4 in tumorigenesis for the first time[46]. Our study and previous studies confirmed that PC4 is highly expressed in lung cancer[47], breast cancer[48], prostate cancer[49], astrocytoma[50] and esophageal squmaous cell carcinoma[51], and regulates cancer growth, lymphatic metastasis, and chemo-radiosensitivity. However, the PC4 role in hematological cancers, including DLBCL are still unknown. Here, we specifically characterized the expression and biological function of PC4 in DLBCL. Through bioinformatics and clinical samples analysis, PC4 was found to be upregulated in DLBCL, positively correlated with c-Myc expression and showed poor prognosis of patients. These results encourage us to further explore the functional significance of increased PC4 expression in DLBCL, especially in c-Myc(+)

DLBCL. Then, in vivo and in vitro studies showed that targeting PC4 could induce autophagic cell death through blocking c-Myc mediated aerobic glycolysis in c-Myc(+) DLBCL.

Autophagic cell death is different from apoptosis, known as type II programmed cell death, which is mainly characterized by the appearance of abundant vacuole enveloping cytoplasm and organelles, and the degradation of various components inside the vacuole via lysosome[15,18]. In response to metabolic stress, including hunger and energy deficiency, autophagy is mainly regulated by mTOR kinase[52]. In recent years, autophagic cell death has gained enormous attention. Suzanne found that combination of the antidepressants maputiline and fluoxetine can induce autophagic cell death in drug-resistant Burkitt's lymphoma[13]. In multiple myeloma, metformin can induce autophagic cell death through the AMPK/mTOR pathway[14]. Furthermore, mTOR inhibitors have been widely used for the treatment of various cancers, and autophagic cell death is one of the main pathways. However, the knowledge of its regulatory mechanism is still insufficient. Galluzzi reported that a rapid reduction in energy charge below a critical limit is likely to trigger the cell death rather than an adaptive autophagic response[11]. As it is well established, that aerobic glycolysis is the main source of energy in cancers[53]. The evaluating index of the DLBCL patients' condition and prognosis, such as lactate dehydrogenase (LDH) activity[54] and 18F-FDG[55] PET/CT, reflect the dependence of DLBCL cells on aerobic glycolysis. Owing to the critical role of c-Myc in aerobic glycolysis, targeting PC4 could block c-Myc mediated aerobic glycolysis and induce autophagic cell death in c-Myc(+) DLBCL. The autophagic cell death induced by PC4 knockdown is a promising therapeutic target for c-Myc (+) DLBCL as a new type of cell death. PC4 could emerge as a drug target site in cancer for c-Myc through upstream regulation.

Conclusion

In the current study, we firstly reported the expression pattern, diagnostic and prognostic value of PC4 in DLBCL. Furthermore, as a direct upstream regulator of c-Myc, targeting PC4 can induce autophagic cell death through blocking c-Myc mediated aerobic glycolysis and energy supply, and activate AMPK / mTOR signaling in c-Myc(+) DLBCL. Therefore, our study provides novel insights into the functions and mechanisms of PC4 in c-Myc(+) DLBCL, and suggest that PC4 may be a novel therapeutic target for c-Myc(+) DLBCL.

Abbreviations

DLBCL: Diffuse large B cell lymphoma; PC4:Positive Cofactor 4; ECAR: Extracellular acidification rate; 2-NBDG:2-[N-(7-nitrobenz-2-oxa-1, 3-diazo-l-4-yl)amino] -2-deoxy-D-glucose; EMSA: Electrophoretic mobility shift assay; TEM: Transmission electron microscopy; ChIP: Chromatin Immunoprecipitation; GO: Gene Ontology; KEGG: Kyoto Encyclopedia of Genes and Genomes; qPCR: Quantitative RT-PCR; DLRTM: Dula-luciferase reporter assay. CCK-8 :Cell Counting Kit-8. BS: Binding site. WT: Wildtype. MT: Mutant type. AV:Autophagic vacuole.

Declarations

Acknowledgements

Not applicable.

Authorship Contributions

LM, QG, PL, JC, and CS conceived and designed the project. LM performed the mostly experiments, analyzed the data, drafted the manuscript; QG and MX contributed to the collection of human tissues; PL took part in animal experiments; PL,ZC and YW and GL took part in cellular and molecular biology experiments, QG and PL, YW, XT, YL and ZC edited the manuscript; CS designed the study, supervised the experiments and revised the manuscript. All authors have read and approved the final manuscript.

Funding

This work was supported by the University Innovation Team Building Program of Chongqing (CXTDG201602020), and intramural research project grants (AWS17J007, and 2018-JCJQ-ZQ-001 and 2020XQN13).

Availability of data and materials

All data generated and analyzed during this study are included in this published article and its additional file.

Ethics approval and consent to participate

The animal study was performed in compliance with relevant regulatory standards, and it was followed the care and use of Guidelines from Laboratory Animals of theThird Military Medical University.

Consent for publication

Not applicable.

Competing interests

The authors declare no conflict of interest and any commercial affiliations.

References

1. Chapuy B, Stewart C, Dunford AJ, Kim J, Kamburov A, Redd RA, Lawrence MS, Roemer MGM, Li AJ, Ziepert M, Staiger AM, Wala JA, Ducar MD, Leshchiner I, Rheinbay E, Taylor-Weiner A, Coughlin CA, Hess JM, Pedamallu CS, Livitz D, Rosebrock D, Rosenberg M, Tracy AA, Horn H, van Hummelen P, Feldman AL, Link BK, Novak AJ, Cerhan JR, Habermann TM, Siebert R, Rosenwald A, Thorner AR, Meyerson ML, Golub TR, Beroukhim R, Wulf GG, Ott G, Rodig SJ, Monti S, Neuberg DS, Loeffler M,

Pfreundschuh M, Trumper L, Getz G, Shipp MA. Molecular subtypes of diffuse large B cell lymphoma are associated with distinct pathogenic mechanisms and outcomes. Nature medicine. 2018, 24(5): 679-690.

2. Jardin F. Improving R-CHOP in diffuse large B-cell lymphoma is still a challenge. The Lancet Oncology. 2019, 20(5): 605-606.
3. Schmitz R, Wright GW, Huang DW, Johnson CA, Phelan JD, Wang JQ, Roulland S, Kasbekar M, Young RM, Shaffer AL, Hodson DJ, Xiao W, Yu X, Yang Y, Zhao H, Xu W, Liu X, Zhou B, Du W, Chan WC, Jaffe ES, Gascoyne RD, Connors JM, Campo E, Lopez-Guillermo A, Rosenwald A, Ott G, Delabie J, Rimsza LM, Tay Kuang Wei K, Zelenetz AD, Leonard JP, Bartlett NL, Tran B, Shetty J, Zhao Y, Soppet DR, Pittaluga S, Wilson WH, Staudt LM. Genetics and Pathogenesis of Diffuse Large B-Cell Lymphoma. N Engl J Med. 2018, 378(15): 1396-1407.
4. Reddy A, Zhang J, Davis NS, Moffitt AB, Love CL, Waldrop A, Leppa S, Pasanen A, Meriranta L, Karjalainen-Lindsberg ML, Norgaard P, Pedersen M, Gang AO, Hogdall E, Heavican TB, Lone W, Iqbal J, Qin Q, Li G, Kim SY, Healy J, Richards KL, Fedoriw Y, Bernal-Mizrachi L, Koff JL, Staton AD, Flowers CR, Paltiel O, Goldschmidt N, Calaminici M, Clear A, Gribben J, Nguyen E, Czader MB, Ondrejka SL, Collie A, Hsi ED, Tse E, Au-Yeung RKH, Kwong YL, Srivastava G, Choi WWL, Evens AM, Pilichowska M, Sengar M, Reddy N, Li S, Chadburn A, Gordon LI, Jaffe ES, Levy S, Rempel R, Tzeng T, Happ LE, Dave T, Rajagopalan D, Datta J, Dunson DB, Dave SS. Genetic and Functional Drivers of Diffuse Large B Cell Lymphoma. Cell. 2017,171, 481–
5. Rosenwald A, Bens S, Advani R, Barrans S, Copie-Bergman C, Elsensohn MH, Natkunam Y, Calaminici M, Sander B, Baia M, Smith A, Painter D, Pham L, Zhao S, Ziepert M, Jordanova ES, Molina TJ, Kersten MJ, Kimby E, Klapper W, Raemaekers J, Schmitz N, Jardin F, Stevens WBC, Hoster E, Hagenbeek A, Gribben JG, Siebert R, Gascoyne RD, Scott DW, Gaulard P, Salles G, Burton C, de Jong D, Sehn LH, Maucort-Boulch D. Prognostic Significance of MYC Rearrangement and Translocation Partner in Diffuse Large B-Cell Lymphoma: A Study by the Lunenburg Lymphoma Biomarker Consortium. Journal of clinical oncology : official journal of the American Society of Clinical Oncology. 2019, 37(35): 3359-3368.
6. Zamani-Ahmadmahmudi M, Nassiri SM. Development of a Reproducible Prognostic Gene Signature to Predict the Clinical Outcome in Patients with Diffuse Large B-Cell Lymphoma. Sci Rep. 2019 Aug 21;9(1):12198.
7. Dang CV. MYC on the path to cancer. Cell. 2012, 149(1): 22-35.
8. Dang CV, Reddy EP, Shokat KM, Soucek L. Drugging the 'undruggable' cancer targets. Nature reviews Cancer. 2017, 17(8): 502-508.
9. Stine ZE, Walton ZE, Altman BJ, Hsieh AL, Dang CV. MYC, Metabolism, and Cancer. Cancer discovery. 2015, 5(10): 1024-1039.
10. Wu H, Liu C, Yang Q, Xin C, Du J, Sun F, Zhou L. MIR145-3p promotes autophagy and enhances bortezomib sensitivity in multiple myeloma by targeting HDAC4. Autophagy. 2020, 16(4): 683-697.

11. Galluzzi L, Green DR. Autophagy-Independent Functions of the Autophagy Machinery. Cell. 2019, 177(7): 1682-1699.
12. Li Hua Dong, Shu Cheng, Zhong Zheng, Li Wang, Yang Shen, Zhi Xiang Shen, Sai Juan Chen and Wei Li Zhao. Histone deacetylase inhibitor potentiated the ability of MTOR inhibitor to induce autophagic cell death in Burkitt leukemia/lymphoma. Journal of Hematology & Oncology. 2013, 6:53.
13. Cloonan SM, Williams DC. The antidepressants maprotiline and fluoxetine induce Type II autophagic cell death in drug-resistant Burkitt's lymphoma. International journal of cancer. 2011, 128(7): 1712-1723.
14. Wang Y, Xu W, Yan Z, Zhao W, Mi J, Li J, Yan H. Metformin induces autophagy and G0/G1 phase cell cycle arrest in myeloma by targeting the AMPK/mTORC1 and mTORC2 pathways. J Exp Clin Cancer Res. (2018) 37:63.
15. Lamy L, Ngo VN, Emre NC, Shaffer AL, 3rd, Yang Y, Tian E, Nair V, Kruhlak MJ, Zingone A, Landgren O, Staudt LM. Control of autophagic cell death by caspase-10 in multiple myeloma. Cancer cell. 2013, 23(4): 435-449.
16. Levy, J. M. M., Towers, C. G. & Thorburn, A. Targeting autophagy in cancer. Nat.Rev. Cancer 17, 528–542 (2017).
17. Sui, X. et al. Autophagy and chemotherapy resistance: a promising therapeutic target for cancer treatment. Cell Death Dis. 4, e838 (2013).
18. Liu S, Lin H, Wang D, Li Q, Luo H, Li G, Chen X, Li Y, Chen P, Zhai B, Wang W, Zhang R, Chen B, Zhang M, Han X, Li Q, Chen L, Liu Y, Chen X, Li G, Xiang Y, Duan T, Feng J, Lou J, Huang X, Zhang Q, Pan T, Yan L, Jin T, Zhang W, Zhuo L, Sun Y, Xie T, Sui X. PCDH17 increases the sensitivity of colorectal cancer to 5-fluorouracil treatment by inducing apoptosis and autophagic cell death. Signal Transduct Target Ther. (2019) 4:53.
19. Saravia J, Raynor JL, Chapman NM, Lim SA, Chi H.Signaling networks in immunometabolism. Cell Res. 2020 Apr;304(4).
20. Dong Yang,Tu Rongfu,Liu Hudan et al. Regulation of cancer cell metabolism: oncogenic MYC in the driver's seat.[J] .Signal Transduct Target Ther, 2020, 5: 124.
21. Hayes JD, Dinkova-Kostova AT, Tew KD. Oxidative Stress in Cancer. Cancer Cell 2020 Aug 10;382(2).
22. Sha Chulin,Barrans Sharon,Cucco Francesco et al. Molecular High-Grade B-Cell Lymphoma: Defining a Poor-Risk Group That Requires Different Approaches to Therapy.[J]. J Clin Oncol, 2019, 37: 202-212.
23. Ge H, Roeder RG. Purification, cloning, and characterization of a human coactivator, PC4, that mediates transcriptional activation of class II genes. Cell. 1994, 78(3): 513-523.
24. Kretzschmar M, Kaiser K, Lottspeich F, Meisterernst M. A novel mediator of class II gene transcription with homology to viral immediate-early transcriptional regulators. Cell. 1994 Aug 12;78(3):525–34.
25. Malik S, Guermah M and Roeder RG. A dynamic model for PC4 coactivator function in RNA polymerase II transcription. Proc Natl Acad Sci USA. 1998; 95: 2192-2197.

26. Tavenet A, Suleau A, Dubreuil G, Ferrari R, Ducrot C, Michaut M, et al. Genome-wide location analysis reveals a role for Sub1 in RNA polymerase III transcription. Proceedings of the National Academy of Sciences of the United States of America. 2009 Aug 25;106(34):14265–70.
27. Calvo O, Manley JL. The transcriptional coactivator PC4/Sub1 has multiple functions in RNA polymerase II transcription. EMBO Journal. 2005 Mar 9;24(5):1009–20.
28. Wang Z, Roeder RG. DNA topoisomerase I and PC4 can interact with human TFIIIC to promote both accurate termination and transcription reinitiation by RNA polymerase III. Molecular Cell. 1998;1(5):749–57.
29. Malik S, Guermah M, Roeder RG. A dynamic model for PC4 coactivator function in RNA polymerase II transcription. Proceedings of the National Academy of Sciences of the United States of America. 1998 Mar 3;95(5):2192–7.
30. Akimoto Y, Yamamoto S, Iida S, Hirose Y, Tanaka A, Hanaoka F, et al. Transcription cofactor PC4 plays essential roles in collaboration with the small subunit of general transcription factor TFIIE. Genes to Cells. 2014 Dec 1;19(12):879–90.
31. Jo J, Hwang S, Kim HJ, Hong S, Lee JE, Lee S-G, et al. An integrated systems biology approach identifies positive cofactor 4 as a factor that increases reprogramming efficiency. Nucleic acids research. 2016 Feb;44(3):1203–15.
32. Zhong L, Wang Y, Kannan P and Tainsky MA. Functional characterization of the interacting domains of the positive coactivator PC4 with the transcription factor AP-2alpha. Gene. 2003; 320: 155-164.
33. Fukuda A, Nakadai T, Shimada M, Tsukui T, Matsumoto M, Nogi Y, Meisterernst M and Hisatake K. Transcriptional coactivator PC4 stimulates promoter escape and facilitates transcriptional synergy by GAL4-VP16. Mol Cell Biol. 2004; 24: 6525-6535.
34. Das C, Hizume K, Batta K, Kumar BR, Gadad SS, Ganguly S, Lorain S, Verreault A, Sadhale PP, Takeyasu K and Kundu TK. Transcriptional coactivator PC4, a chromatin-associated protein, induces chromatin condensation. Mol Cell Biol. 2006; 26: 8303-8315.
35. Garavis M and Calvo O. Sub1/PC4, a multifaceted factor: from transcription to genome stability. Curr Genet. 2017; 63: 1023-1035.
36. Qiu Q, Basak A, Mbikay M, Tsang BK, Gruslin A. Role of pro-IGF-II processing by proprotein convertase 4 in human placental development. Proc. Natl. Acad. Sci. U.S.A. 2005 Aug 02;102(31).
37. Garavís M, González-Polo N, Allepuz-Fuster P, Louro JA, Fernández-Tornero C, Calvo O. Sub1 contacts the RNA polymerase II stalk to modulate mRNA synthesis. Nucleic acids research. 2017 Mar;45(5):2458–71.
38. Garavís M, Calvo O. Sub1/PC4, a multifaceted factor: from transcription to genome stability. Current Genetics. 2017 Dec; 636(6).
39. Mortusewicz O, Evers B, Helleday T. PC4 promotes genome stability and DNA repair through binding of ssDNA at DNA damage sites. Oncogene. 2016 Feb 11;35(6):761–70.
40. Mortusewicz O, Roth W, Li N, Cardoso MC, Meisterernst M, Leonhardt H. Recruitment of RNA polymerase II cofactor PC4 to DNA damage sites. Journal of Cell Biology. 2008 Dec 1;183(5):769–

76.
41. Yu L, Volkert MR. Differential Requirement for SUB1 in Chromosomal and Plasmid Double-Strand DNA Break Repair. PLoS ONE. 2013 Mar 12;8(3).
42. Wang J-Y, Sarker AH, Cooper PK, Volkert MR. The Single-Strand DNA Binding Activity of Human PC4 Prevents Mutagenesis and Killing by Oxidative DNA Damage. Molecular and Cellular Biology. 2004 Jul 1;24(13):6084–93.
43. Lejault P, Moruno-Manchon JF, Vemu SM, Honarpisheh P, Zhu L, Kim N, Urayama A, Monchaud D, McCullough LD, Tsvetkov AS. Regulation of autophagy by DNA G-quadruplexes. Autophagy. 2020 May 18.
44. Moruno-Manchon JF, Lejault P, Wang Y, McCauley B, Honarpisheh P, Morales Scheihing DA, Singh S, Dang W, Kim N, Urayama A, Zhu L, Monchaud D, McCullough LD, Tsvetkov AS. Small-molecule G-quadruplex stabilizers reveal a novel pathway of autophagy regulation in neurons. Elife. 2020 Feb 11;9.
45. Sikder Sweta,Kumari Sujata,Mustafi Pallabi et al. Nonhistone human chromatin protein PC4 is critical for genomic integrity and negatively regulates autophagy.[J] .FEBS J, 2019, 286: 4422-4442..
46. Shi C, Mai Y, Zhu Y, Cheng T, Su Y. Spontaneous transformation of a clonal population of dermis-derived multipotent cells in culture. In Vitro Cell Dev Biol Anim. 2007;43:290–6.
47. Peng Y, Yang J, Zhang E, Sun H, Wang Q, Wang T, Su Y, Shi C. Human positive coactivator 4 is a potential novel therapeutic target in non-small cell lung cancer. Cancer Gene Ther. 2012;19:690–6.
48. Luo P, Zhang C, Liao F, Chen L, Liu Z, Long L, Jiang Z, Wang Y, Wang Z, Liu Z, Miao H, Shi C. Transcriptional positive cofactor 4 promotes breast cancer proliferation and metastasis through c-Myc mediated Warburg effect. Cell communication and signaling. (2019) 17:36.
49. Chakravarthi BVSK, Goswami MT, Pathi SS, Robinson AD, Cieślik M, Chandrashekar DS, et al. MicroRNA-101 regulated transcriptional modulator SUB1 plays a role in prostate cancer. Oncogene. 2016 Dec 8;35(49):6330–40.
50. Chen L, Du C, Wang L, Yang C, Zhang JR, Li N, Li Y, Xie XD and Gao GD. Human positive coactivator 4 (PC4) is involved in the progression and prognosis of astrocytoma. J Neurol Sci 2014; 346: 293-298.
51. Qian D, Zhang B, Zeng XL, Le Blanc JM, Guo YH, Xue C, Jiang C, Wang HH, Zhao TS, Meng MB, Zhao LJ, Hao JH, Wang P, Xie D, Lu B and Yuan ZY. Inhibition of human positive cofactor 4 radiosensitizes human esophageal squmaous cell carcinoma cells by suppressing XLF-mediated nonhomologous end joining. Cell Death Dis 2014; 5: e1461.
52. Jia J, Abudu YP, Claude-Taupin A, Gu Y, Kumar S, Choi SW, Peters R, Mudd MH, Allers L, Salemi M, Phinney B, Johansen T, Deretic V. Galectins control MTOR and AMPK in response to lysosomal damage to induce autophagy. Autophagy. 2019, 15(1): 169-171.
53. Hardie DG, Ross FA, Hawley SA. AMPK: a nutrient and energy sensor that maintains energy homeostasis. Nature reviews Molecular cell biology. 2012, 13(4): 251-262.
54. Zhong H, Chen J, Cheng S, Chen S, Shen R, Shi Q, Xu P, Huang H, Zhang M, Wang L, Wu D, Zhao W. Prognostic nomogram incorporating inflammatory cytokines for overall survival in patients with

aggressive non-Hodgkin's lymphoma. EBioMedicine 2019, 41: 167-174.

55. Shagera QA, Cheon GJ, Koh Y, Yoo MY, Kang KW, Lee DS, Kim EE, Yoon SS, Chung JK. Prognostic value of metabolic tumour volume on baseline (18)F-FDG PET/CT in addition to NCCN-IPI in patients with diffuse large B-cell lymphoma: further stratification of the group with a high-risk NCCN-IPI. European journal of nuclear medicine and molecular imaging. 2019, 46(7): 1417-1427.

Table

Table 1. Correlations between c-Myc expression level and clinic characteristics of patients with DLBCL.

Clinicopathological parameters	patients Number (%)	c-Myc Negative (%)	Positive (%)	P Value
All cases	54(100)	27(50)	27(50)	P=1.000
Gender				
Female	27(50)	12(22.2)	15(27.8)	P=0.587
Male	27(50)	15(27.8)	12(22.2)	
Age				
< 60	37(31.5)	19(35.2)	18(33.3)	P=1.000
≥ 60	17(68.5)	8(14.8)	9(16.7)	
Subtype				
GCB type	29(53.7)	17(31.5)	12(22.2)	P=0.243
Non-GCB type	22(40.7)	8(14.8)	14(25.9)	
Unclassified DLBCL	3(5.6)	2(3.7)	1(1.9)	
Ki-67 expression				
≥ 70%	22(40.7)	8(14.8)	14(25.9)	P=0.097
< 70	32(59.3)	19(35.2)	13(24.1)	
Ann Arbor stage				
I-II	17(31.5)	16(29.6)	1(1.9)	P=0.000
III-IV	37(68.5)	11(20.4)	26(48.1)	
Time from enrollment		Event-free survival (standard error)		
12 months	66.7(6.7)	92.6(2.1)	77.8(4.4)	P=0.000
24 months	63.0(7.3)	92.6(2.1)	74.1(5.1)	P=0.000

Corrected with continuity correction of Pearson's χ^2 test.DLBCL：Diffuse large B-cell lymphoma；

Figures

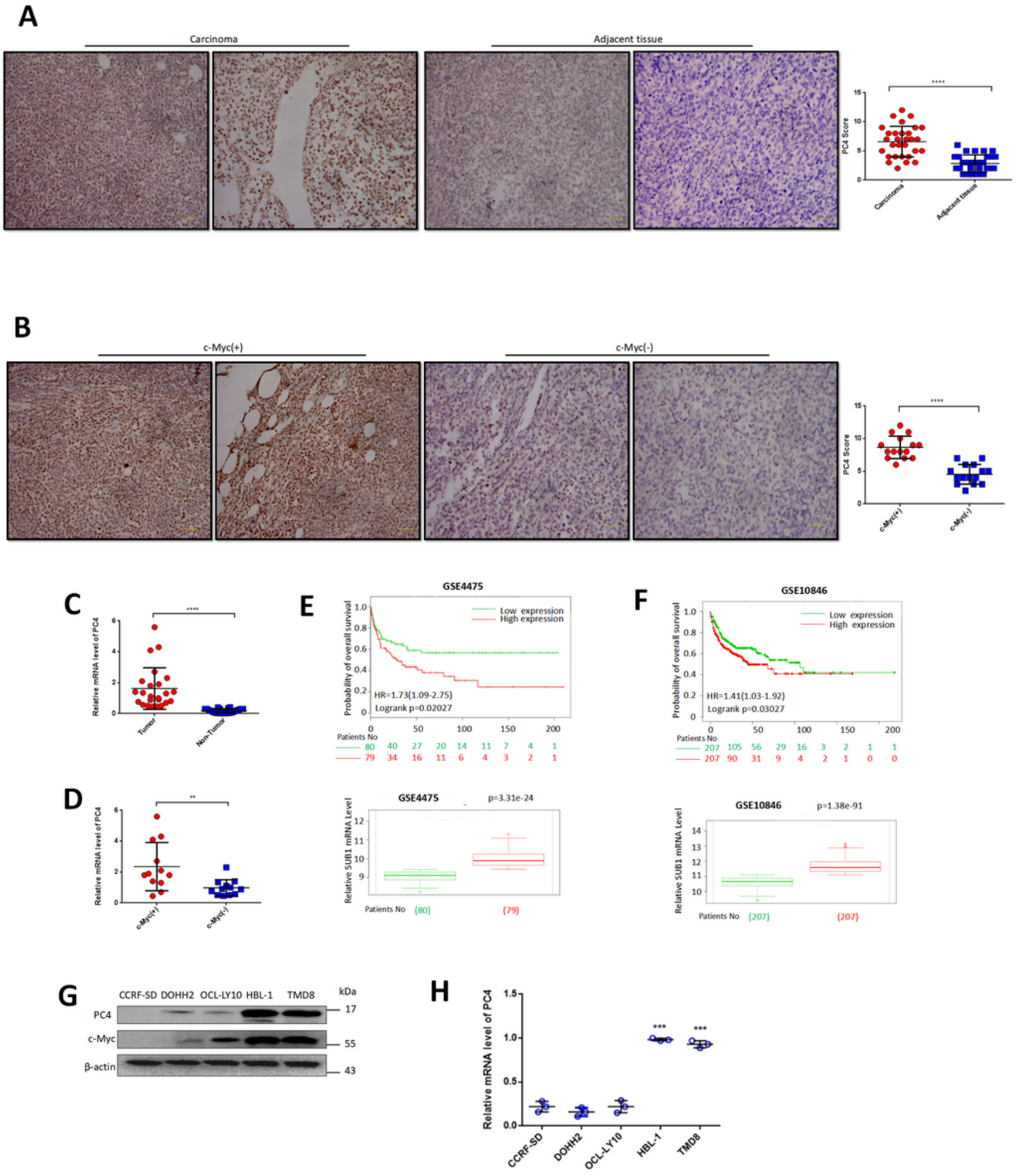

Figure 1

PC4 is significantly up-regulated in diffuse large B-cell lymphoma with c-Myc expression patients and cell lines,and is correlated with poor prognosis of patients. (A) Immunohistochemical staining for PC4 protein in DLBCL tissues (n=30) and adjacent tissues. Scale bar represents 50um. (B) Immunohistochemical staining of PC4 in c-Myc(+)(n=15) and c-Myc(-)(n=15) of DLBCL tissues. Scale bar represents 50um. (C) The mRNA level of PC4 in DLBCL patients' tissues (n=24) and normal tissues (n=24). (D) The mRNA level of PC4 in c-Myc(+)(n=12) and c-Myc(-)(n=12) DLBCL patients' tissues. (E) Kaplan-Meier analysis for the association of PC4 expression levels with overall survival time in DLBCL(n=159). (F) Kaplan-Meier analysis for the association of PC4 expression levels with overall survival time in DLBCL(n=417). (G) The protein level of PC4 and c-Myc in CCRF-SD cells and DLBCL cell Lines. (H) The mRNA level of PC4 in CCRF-SD cells and DLBCL cell Lines. All data are represented as mean ±SD. **p<0.01, ***p<0.001, ****p<0.0001.

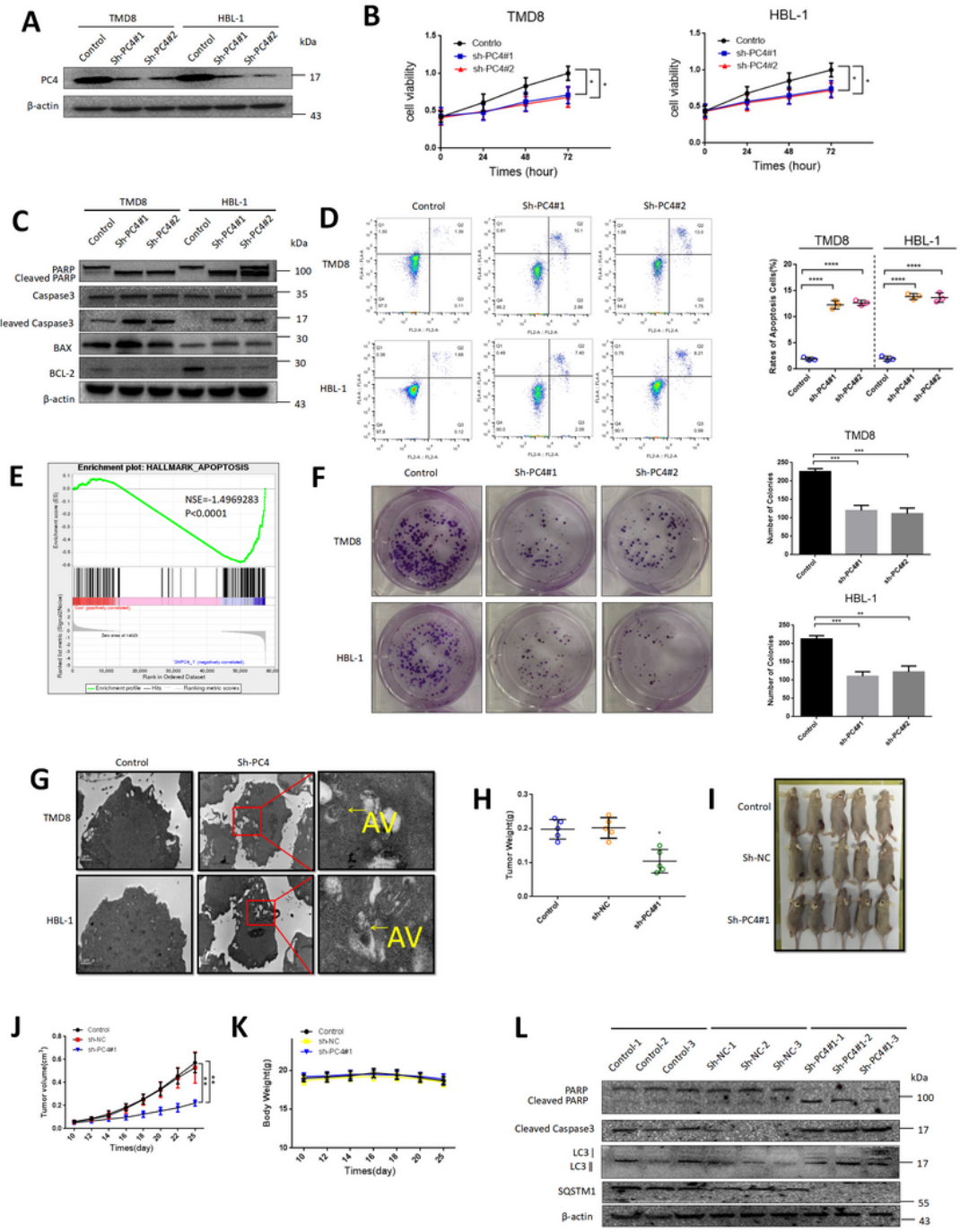

Figure 2

Knockdown of PC4 induces cell apoptosis in MYC-expressing DLBCL in vitro and in vivo. (A) Two shRNAs (shPC4#1 and shPC4#2) were used to establish the stable PC4 knockdown cell lines. The PC4 knockout efficiency was examined by western blot.(B) Cell viability in the constructed cells was determined by CCK-8 assay. (C) The expression of apoptosis markers (c-caspase 3, PARP, Bax and Bcl-2) was detected by western blotting in the constructed cells. (D) Apoptosis rate in the constructed cells was determined by

flow cytometry. (E) GSEA comparing the gene sets of APOPTOSIS in the constructed TMD8 cells. (F) The clone formation assay of the constructed cells. (G) The constructed cells were observed by TEM. (J) The TMD8 cell with stable PC4-knockdown was inoculated into athymic male nude mice. At the endpoint, the xenografts were photographed (I) dissected and weighed (H). (K) The body weight of the mice was measured. (L) LC3,SQSTM1 and PARP,c-Caspase3 was detected by western blotting in dissected xenografts. All data indicate the mean ±SD. *p<0.05, **p<0.01, ***p<0.001, ****p<0.0001.

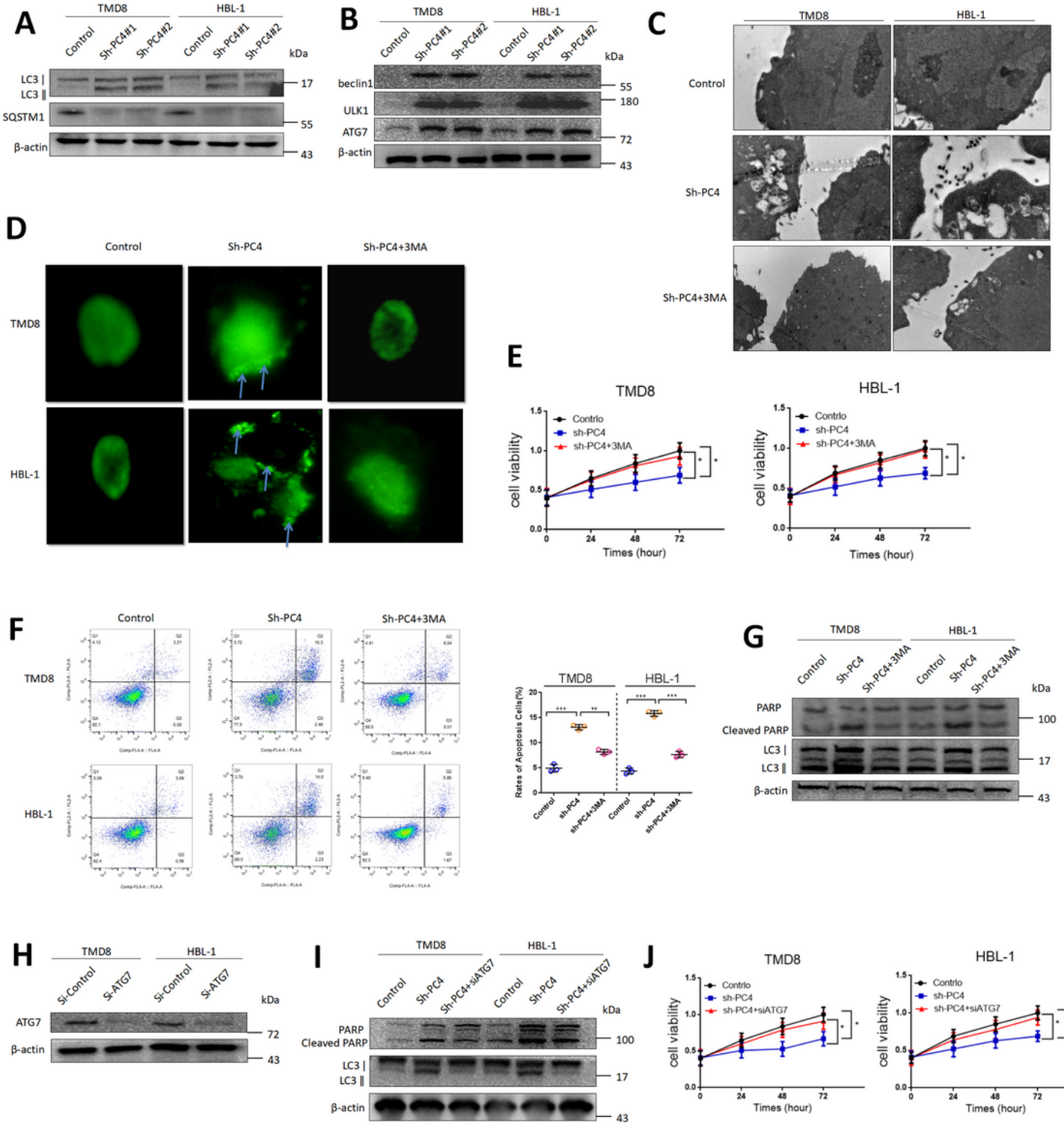

Figure 3

Inhibition of PC4 induces apoptosis in MYC-expressing DLBCL by inducing excessive autophagy. (A) The expression of LC3 and SQSTM1 was detected by western blotting in the constructed cells. (B) The protein level of beclin1, ULK1 and ATG7 was detected by western blotting in the constructed cells. (C) The constructed cells with or without 3MA (4mM) were observed for autophagy using TEM. (D) The constructed cells were transfected with a GFP-LC3 plasmid, The formation of GFP-LC3 puncta was observed using immunofluorescence. (E) Cell viability in the constructed cells was determined by CCK-8 assay. (F) Apoptosis rate in the constructed cells was determined by flow cytometry. (G) The expression of LC3 and PARP was detected by western blotting in the constructed cells. (H) TMD8 and HBL-1 cells were transfected using siRNA against Atg7, and Atg7 expression and LC3,PARP(I) was detected using western blotting. (J) Cell viability in the constructed cells was determined by CCK-8 assay. All data are represented as mean ±SD. *$p<0.05$, **$p<0.01$, ***$p<0.001$.

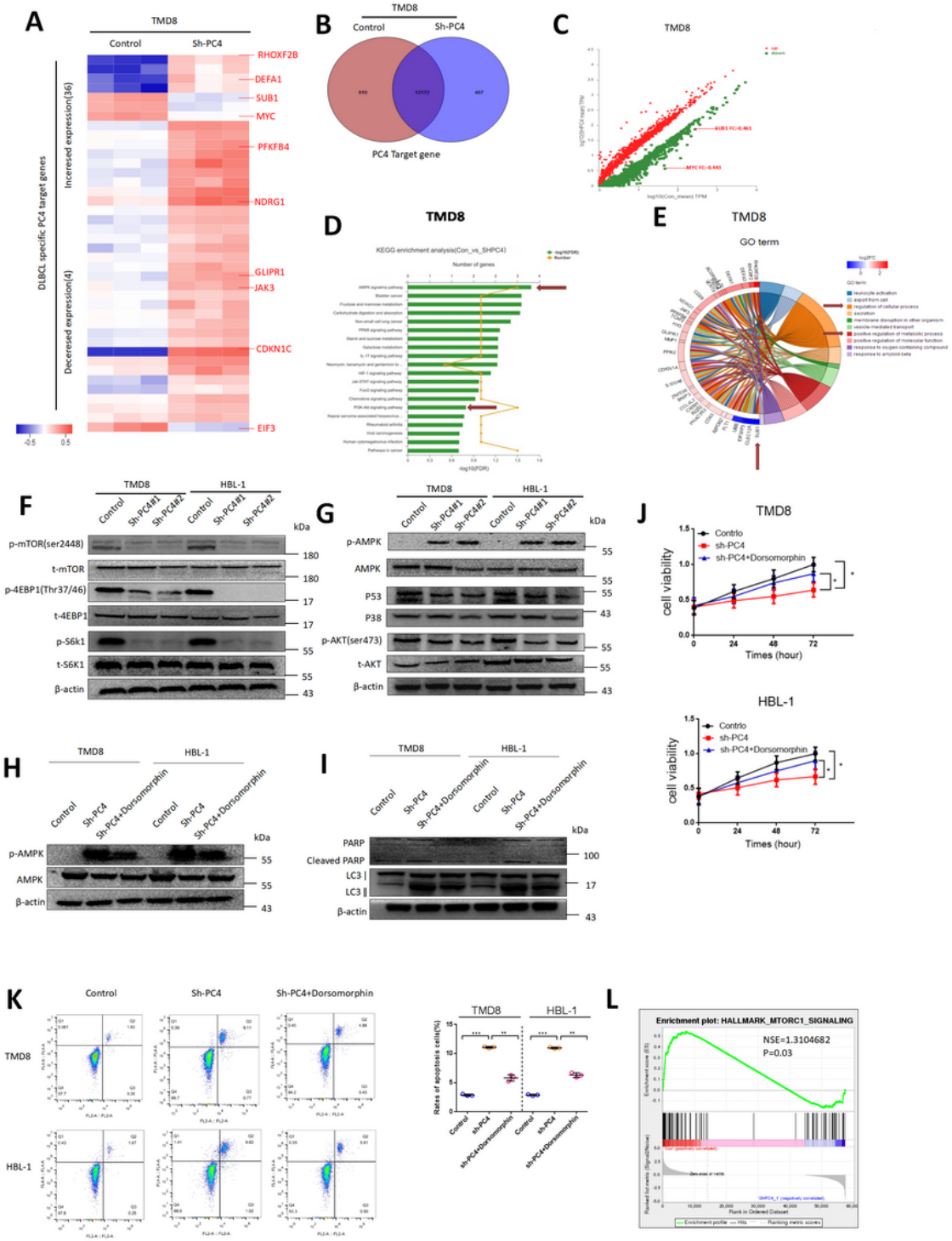

Figure 4

Knockdown of PC4 induces apoptosis in MYC-expressing DLBCL by inducing excessive autophagy. (A) Heat maps show mRNA levels of target genes in the constructed cells. (B) Venn diagram in the constructed cells. (C) Statistics of expression difference in the constructed cells. (D) KEGG enrichment analysis in the constructed cells.(E) GO analysis in the constructed cells. (F) The mTOR and AMPK (G) and their related protein was detected by western blotting in the constructed cells. (H) The AMPK and

LC3,PARP(I) was detected by western blotting in the constructed cells with or without Dorsomorphin treatment. (J) Cell viability in the constructed cells were determined by CCK-8 assay. (K) Apoptosis rate in the constructed cells by flow cytometry. (L) GSEA comparing the gene sets of MTORC1 in the constructed TMD8 cells. All data are represented as mean ±SD. *p<0.05, **p<0.01, ***p<0.001.

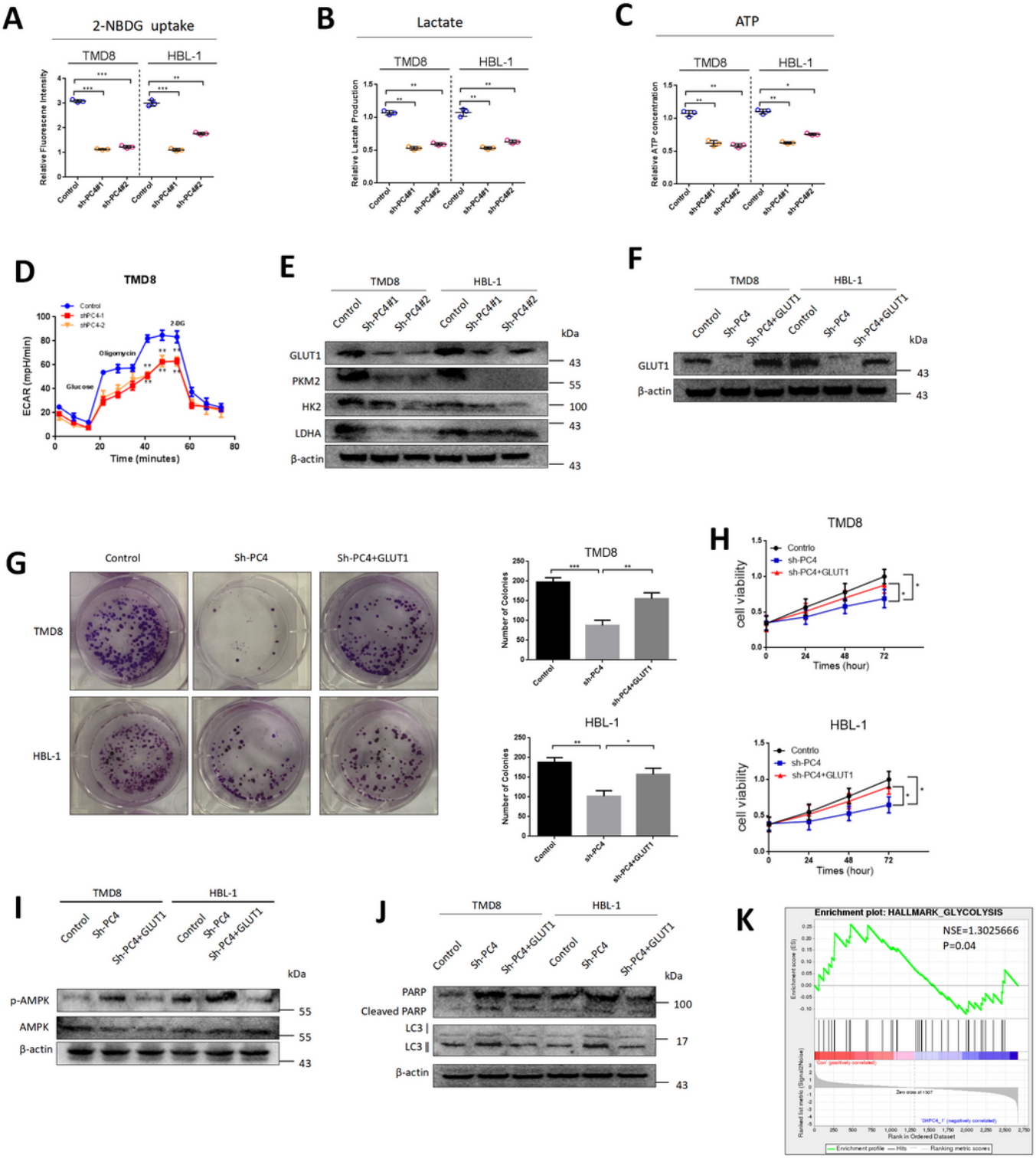

Figure 5

Knockdown of PC4 induces excessive autophagy through inhibition of glycolysis metabolism in MYC-expressing DLBCL. (A) 2-NBDG uptake, (B) Lactate and (C) ATP were determined in the constructed cells. (D) ECAR was determined in PC4 knockdown TMD8 cells. (E) The expression of GLUT1, PKM2, HK2 and LDHA were detected by western blotting in the constructed cells. (F) the protein levels of GLUT1 were detected by western blotting after overexpression of GLUT1. (G) The clone formation assay of the constructed cells. (H) Cell viability in the constructed cells was determined by CCK-8 assay. (I) The AMPK and LC3,PARP(J) was detected by western blotting. (K) GSEA comparing the gene sets of GLYCOLYSIS in the constructed TMD8 cell lines. All data are represented as mean ±SD. *p<0.05, **p<0.01, ***p<0.001.

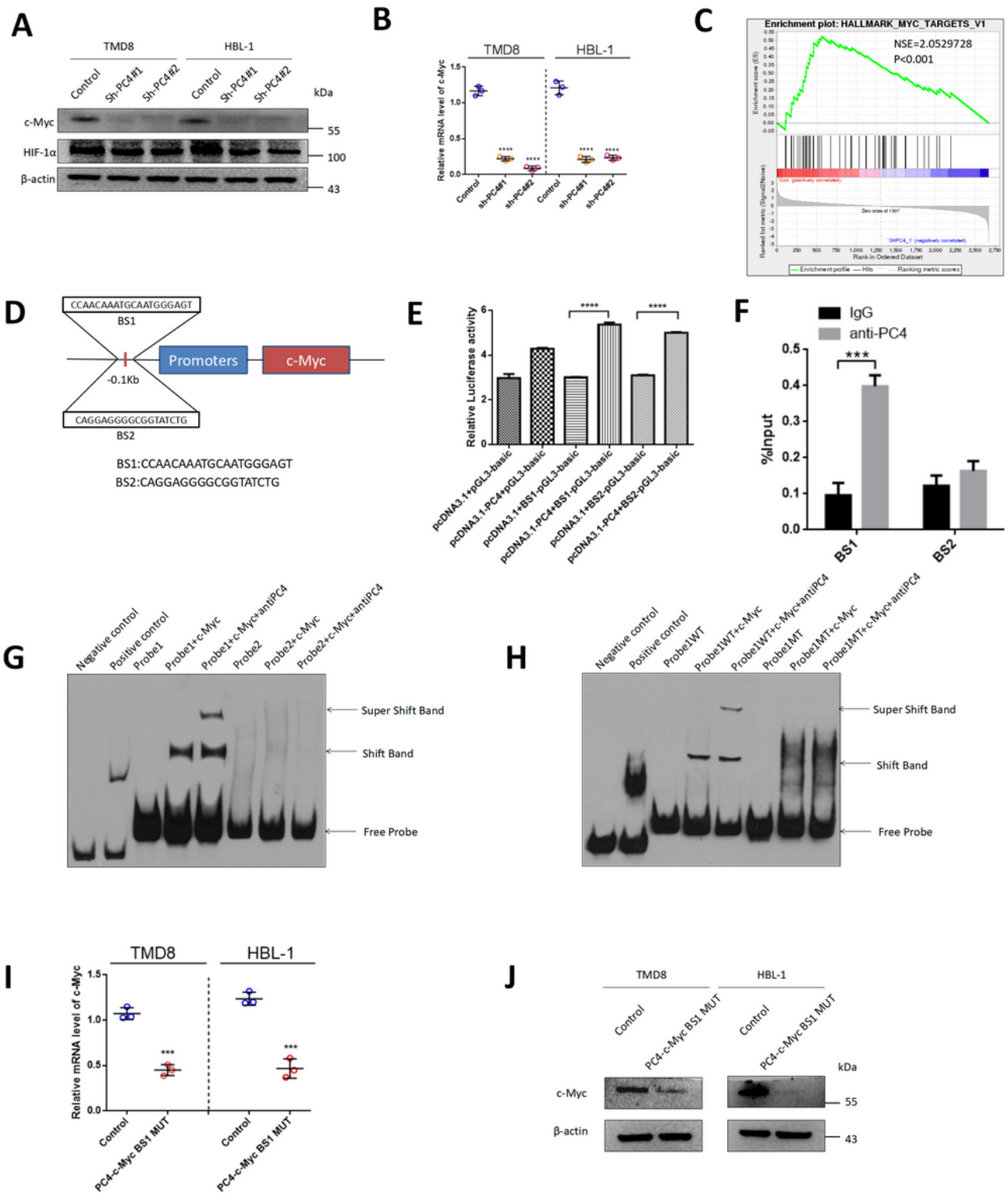

Figure 6

PC4 directly regulates c-Myc transcription by binding to c-Myc's promoters. (A) The Protein levels of c-Myc and HIF-1α were detected by western blotting. (B) The mRNA levels of c-Myc were detected by qPCR. (C) GSEA comparing the gene sets of MYC in the constructed TMD8 cells. (D)Schematic presentation of PC4 and c-Myc binding sites on the c-Myc locus. (E) Luciferase reporter activities were assessed in c-Myc promoter along with or without co-expressing PC4. (F) ChIP-PCR analysis for the PC4 occupancy in the c-

Myc promoters in TMD8 cells. (G) EMSA was conducted to detect the binding of PC4 to c-Myc's promoters. (H) EMSA were conducted to detect the BS1 binding sites of PC4 to c-Myc's promoters. (I) The mRNA levels and protein levles(J) of c-Myc were detected in PC4-c-Myc BS1 MUT cell lines and controls. All data are represented as mean ±SD. ***p<0.001, ****p<0.0001.

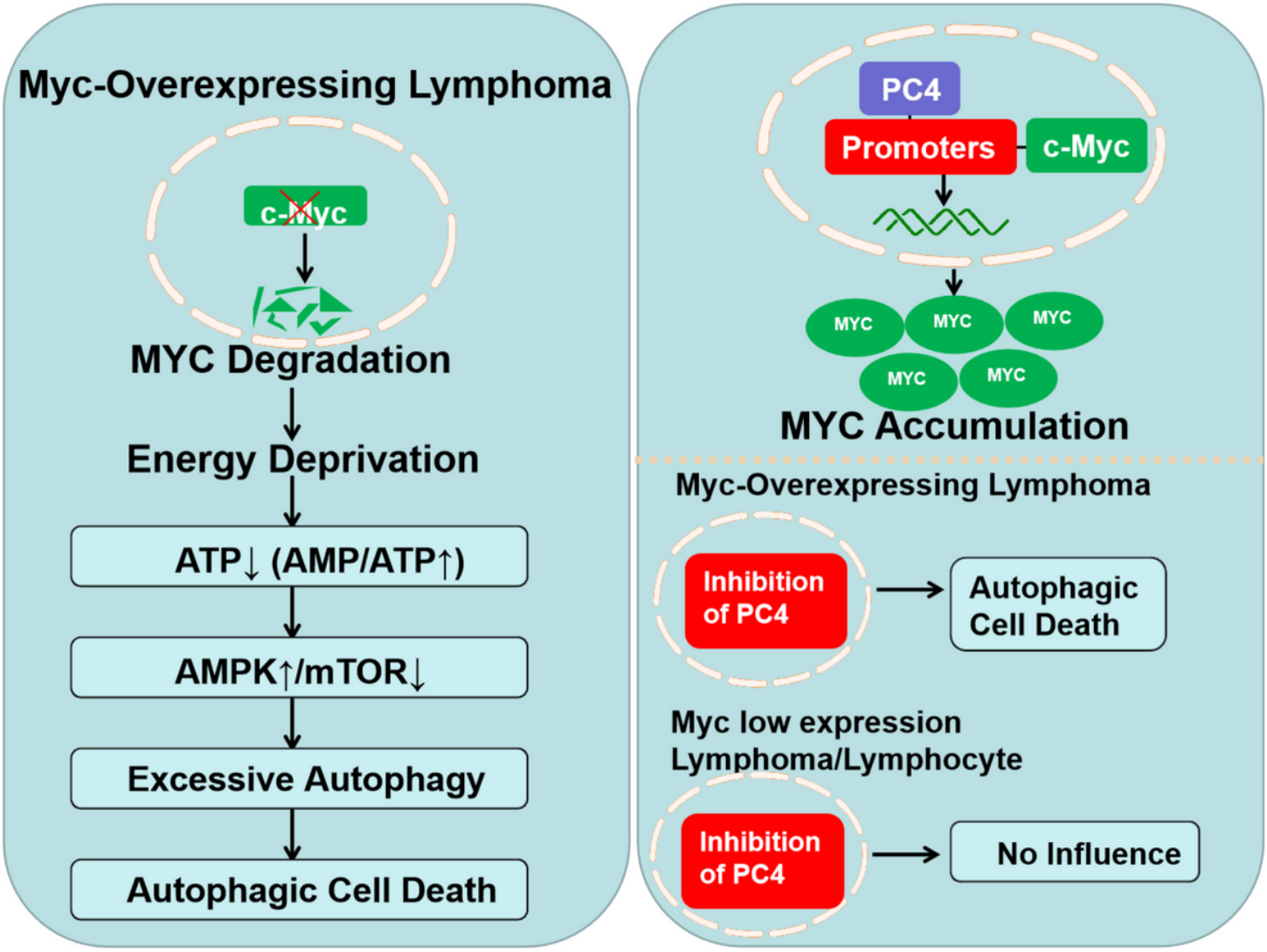

Figure 7

Schematic illustration for the potential mechanisms of PC4 in diffuse large B-cell lymphoma progression. In c-Myc(+) DLBCL, PC4 directly regulated the c-Myc transcription by binding to c-Myc's promoters, targeting PC4 induced autophagic cell death through Inhibited their glycometabolism.

Supplementary Files

This is a list of supplementary files associated with this preprint. Click to download.

- Additionalfile.pdf